ELSEVIER

Biochimica et Biophysica Acta 1561 (2002) 47–64

BIOCHIMICA ET BIOPHYSICA ACTA
BBA

www.bba-direct.com

Review

Structure and association of ATP-binding cassette transporter nucleotide-binding domains

Ian D. Kerr *

Nuffield Department of Clinical Laboratory Sciences, University of Oxford, Level 4, John Radcliffe Hospital, Oxford OX3 9DS, UK

Received 20 September 2001; accepted 12 November 2001

Abstract

ATP-binding cassette transporters are responsible for the uptake and efflux of a multitude of substances across both eukaryotic and prokaryotic membranes. Members of this family of proteins are involved in diverse physiological processes including antigen presentation, drug efflux from cancer cells, bacterial nutrient uptake and cystic fibrosis. In order to understand more completely the role of these multidomain transporters an integrated approach combining structural, pharmacological and biochemical methods is being adopted. Recent structural data have been obtained on the cytoplasmic, nucleotide-binding domains of prokaryotic ABC transporters. This review evaluates both these data and the conflicting implications they have for domain communication in ABC transporters. Areas of biochemical research that attempt to resolve these conflicts will be discussed. © 2002 Elsevier Science B.V. All rights reserved.

Keywords: ABC transporter; Nucleotide-binding domain; Structure; P-glycoprotein; Domain interaction

1. Introduction

Elucidation of the sequence of prokaryotic and eukaryotic genomes has allowed us to confirm that about 30% of encoded proteins are membrane spanning. Within this complement the largest family in many genomes is the ATP-binding cassette (ABC) transporter family. ABC transporters can act as exporters, importers, receptors and channels and mediate a plethora of physiological phenomena [1]. An overview of this diversity is provided in Table 1, although more complete descriptions of particular ABC transporters can be found in two recent review series [2,3]. Detailed analysis of ABC transporters within the sequenced genomes of organisms can be found in several recent papers [4–8]. ABC transporters appear to be minimally composed of four domains (Fig. 1), viz two membrane-spanning domains (MSDs) and two nucleotide-binding domains (NBDs). The MSDs are presumed to span the membrane multiple times in the form of α-helices, although no definitive demonstration of this has been provided for any ABC transporter. An alternative β-barrel-based hypothesis has been presented for

Abbreviations: ABC, ATP-binding cassette; NBD, nucleotide-binding domain; MSD, membrane-spanning domain; PBP, periplasmic binding protein; SMC, structural maintenance of chromosomes; P-gp, P-glycoprotein; TAP, transporter associated with antigen presentation; MRP, multidrug resistance associated protein; SUR, sulphonylurea receptor; SASA, solvent accessible surface area; CHAPS, 3-[(3-cholamidopropyl)dimethylammonio]-1-propanesulphonate; MIANS, 2-(4′-maleimidylanilino)naphthalene-6-sulphonic acid; FRET, fluorescence resonance energy transfer

* Fax: +44-1865-22-18-34.
E-mail address: kerrid@icrf.icnet.uk (I.D. Kerr).

0005-2736/02/$ – see front matter © 2002 Elsevier Science B.V. All rights reserved.
PII: S0304-4157(01)00008-9

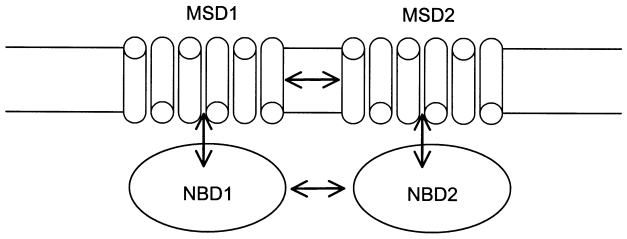

Fig. 1. Schematic representation of ABC transporter membrane topology. Transporters typically contain two intracellular nucleotide-binding domains (NBDs) and two multiple membrane-spanning domains (MSDs). The double-headed arrows indicate domain:domain communication sites that regulate ABC transporter activity.

their secondary structure [9]. The MSDs form the pathway for the transported substrate (or 'allocrite' [10]) and, consistent with this, a number of pharmacological studies have pinpointed the MSDs as containing binding sites for allocrites (e.g. [11]). The NBDs are responsible for ATP hydrolysis and for coupling energy release to allocrite transport [10].

The four domains may be encoded as separate polypeptides, as is the case for a considerable number of bacterial transporters (e.g. $HisQMP_2$, Table 1), or be contained within a single polypeptide chain, as is the case for the majority of eukaryotic ABC transporters (e.g. P-glycoprotein, Table 1). Various intermediates between these extremes are also observed. For example, the two NBDs may be fused together in a single polypeptide, as is the case for the bacterial ribose transporter (RbsA), or the whole transporter may be associated from two 'half-transporters' in which each MSD is fused to an NBD (e.g. TAP1/2, Table 1). In addition to the four core domains a number of ABC transporters have additional domains. In prokaryotic uptake systems this is normally in the form of a periplasmic binding protein (PBP) which has a high affinity for the allocrite and which interacts with the MSDs to effect transmembrane allocrite flux (e.g. HisJ, Table 1) [12,13]. An example of an additional domain in a eukaryotic ABC transporter is the regulatory (R) domain of the cystic fibrosis transmembrane conductance regulator (CFTR), which is located between the two homologous halves of the transporter [14].

The ability to mediate vectorial transport of allocrites requires intricate coupling between the MSDs and NBDs (and the periplasmic binding proteins where applicable). One of the recent focuses of ABC transporter research has been to gain insights into this inter-domain communication by both biochemical (e.g. mutagenesis, fluorescence energy resonance) and structural studies. A mechanistic model of inter-domain communication is the catalytic cycle model proposed for P-glycoprotein [15] and which may be generally relevant to ABC transporters. In this model, the two NBDs are alternately catalytic and, therefore, at any given point in the cycle may adopt slightly different conformations. This model has been substantiated in a number of recent studies on eukaryotic transporters [16–19]. A structural basis for the alternating-sites model will only be achieved by determining three types of inter-domain communication (Fig. 1): (i) MSD:MSD interactions which may influence binding and release of allocrites, (ii) NBD:MSD interactions which are proposed to mediate the coupling of nucleotide hydrolysis with allocrite transport, and (iii) NBD:NBD interactions, de-

Table 1
Functions of ABC transporters

Transporter	Organism	Organisation[a]	Allocrite	Ref.
P-glycoprotein	*Homo sapiens*	$(MSD\text{-}NBD)_2$	Hydrophobic drugs	[67]
LmrA	*Lactococcus lactis*	2(MSD-NBD)	Hydrophobic drugs	[68]
CFTR	*H. sapiens*	$(MSD\text{-}NBD)_2$	Chloride ion	[14]
HylB	*Staphylococcus aureus*	2(MSD-NBD)	Haemolysin	[69]
ABCA4	*H. sapiens*	$(MSD\text{-}NBD)_2$	Retinoids	[70]
$HisQMP_2J$	*S. typhimurium*	5 polypeptides	Histidine	[35]
$MalFGK_2E$	*E. coli*	5 polypeptides	Maltose	[38]
TAP1/2	*H. sapiens*	2(MSD-NBD)	Antigenic peptides	[71]

[a]$(MSD\text{-}NBD)_2$ indicates a single polypeptide containing two transmembrane domains and two NBDs. 2(MSD-NBD) indicates two polypeptides each containing a single MSD and a single NBD.

termination of which is essential to understanding the communication between the two homologous halves of an ABC transporter.

The interaction between NBDs is the prime concern of this review as it is believed that a common inter-domain communication may exist in transporters of unrelated function. This hypothesis stems from the fact that NBDs show considerably more sequence identity across the spectrum of ABC transporters than do the MSDs. Such sequence identity is consistent with the principle that the MSDs form the pathway for allocrite transport, while the NBDs perform the common task of powering this transport. Observations ranging from prokaryotes to eukaryotes indicate that the percentage identity of NBDs is over 25%, suggesting that in transporters of unrelated function the structure of the NBDs is maintained. The sequence conservation is most marked in five regions (Fig. 2). Two of these five motifs (Walker-A and Walker-B) are present in the vast majority of ATP-binding proteins [20] and their sequences are characteristic of this function. The other three motifs, 'Signature Motif', 'Histidine Loop' [4], and 'Glutamine Loop' [21], are more specific and define an ABC transporter NBD. The Signature Motif[1] has received considerable attention in mutagenesis studies because of its remarkable conservation and proposed role in inter-domain communication (see below). The Glutamine Loop, containing a well-conserved glutamine residue at position 113 in the alignment, is located between the Walker-A and Signature Motifs in an otherwise less well conserved region. The final conserved motif in the alignment is the Histidine Loop, situated 30–40 amino acids C-terminal to the Walker-B motif, and containing an almost invariant histidine at position 242. Indeed, all ABC transporters contain a histidine residue in this position in at least one of their two NBDs. An additional conserved element may be the aromatic amino acid residue at position 24 in the alignment (i.e. N-terminal to the Walker-A motif), which structural studies suggest is involved in nucleotide binding (see below) [22]. Within this review the terms Walker-A, Walker-B, Signature Motif, His-Loop and Gln-Loop will be employed to refer to these five sequence motifs.

The role of several of the residues within these motifs has been identified through mutagenesis studies and further elucidated with the advent of the structural studies described below. A complete description is beyond the scope of this review, although an analysis of NBD mutations can be found at the website: http://oxygen.jr2.ox.ac.uk/ian/nbd_mutations.html. In spite of the progress towards understanding NBD structure:function relationships and the assembly of ABC transporter complexes as a whole that continues to be made by biochemical studies, it is clear that detailed high resolution structures are required to make further progress.

2. The monomeric structure of bacterial nucleotide-binding domains

The first description of an NBD structure appeared in 1998 [23] when Stauffacher and colleagues determined the structure of the N-terminal half of the *Escherichia coli* RbsA protein. This protein contains two NBDs within a single polypeptide and the structure elucidated corresponds to the first NBD with some amino acids that presumably correspond to a linker region situated between the N- and C-terminal NBDs. At the time of writing, a complete publication on the RbsA structure has yet to appear. The structure of RbsA was followed by another bacterial NBD structure, namely the HisP protein from *Salmonella typhimurium* [22], which was solved to a resolution of 1.5 Å by Kim and colleagues. HisP contains a single NBD domain and in the assembled histidine transport complex is associated as a homodimer with the membrane-spanning proteins HisQ and HisM [24]. The structure of a monomeric HisP molecule is shown in Fig. 3A. The NBD domain is characterised by three subdomains, an F1-ATPase like subdomain [20], and two ABC-specific smaller subdomains, one of which is predominantly α-helical, the other an antiparallel β-sheet [25]. It is convenient though to visualise the HisP NBD as a rather stubby L-shape, with two distinct 'arms'. Arm-I contains the F1-ATPase-like subdomain in which the Walker-A motif forms a typical phosphate-binding loop (P-loop [20]), together with the Walker-B motif.

[1] The Signature Motif has also been termed the 'linker peptide' and the 'Walker-C' motif.

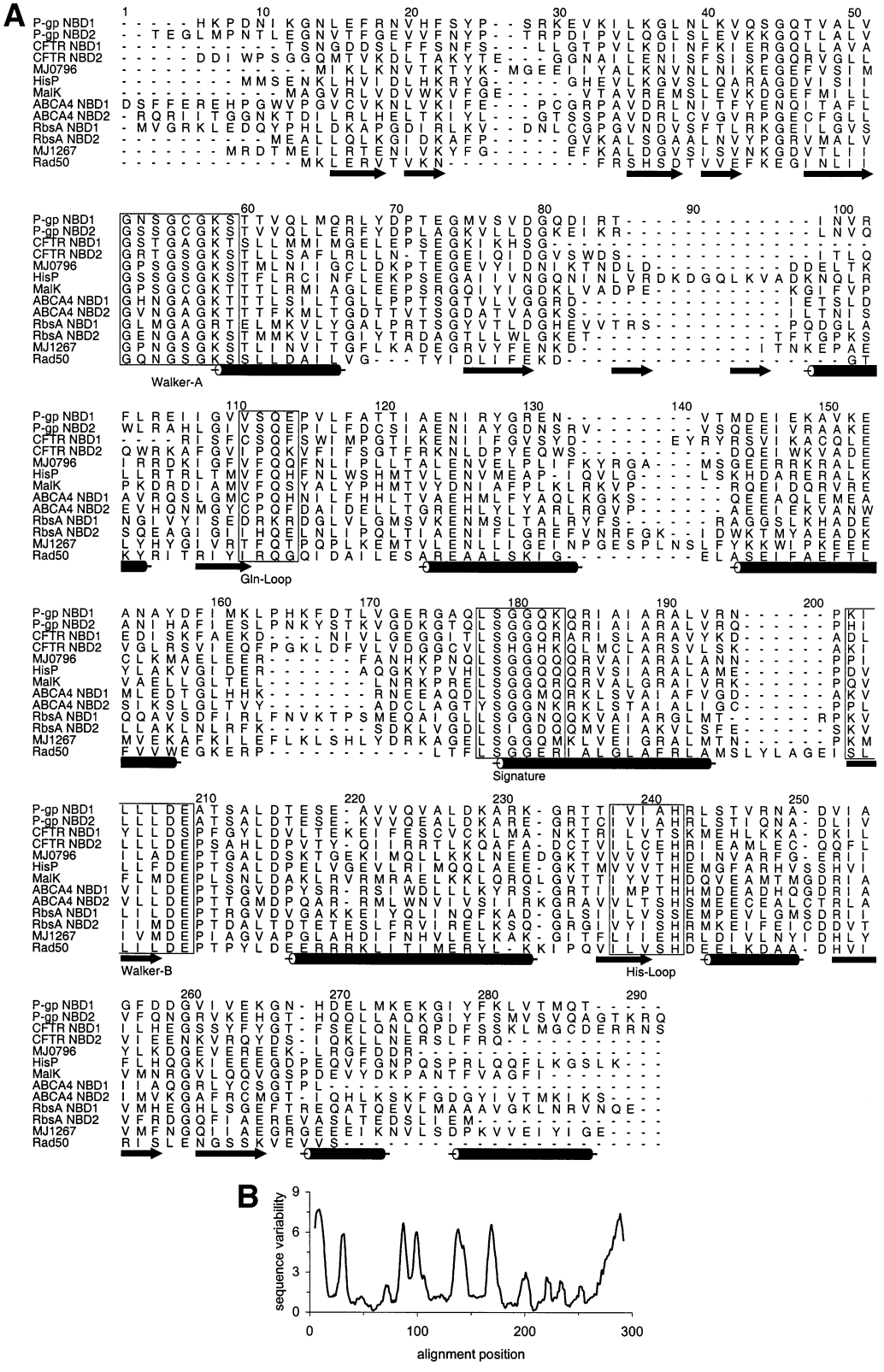
A
P-gp NBD1
P-gp NBD2
CFTR NBD1
CFTR NBD2
MJ0796
HisP
MalK
ABCA4 NBD1
ABCA4 NBD2
RbsA NBD1
RbsA NBD2
MJ1267
Rad50
Walker-A
Gln-Loop
Signature
Walker-B
His-Loop
B
sequence variability
alignment position

Fig. 2. (A) Sequence alignment of NBDs of eukaryotic and prokaryotic ABC transporters. The five conserved motifs are boxed and indicated, while the secondary structural elements in the crystal structure of HisP [22] are displayed as schematic α-helices and β-strands (cylinders and arrow respectively). Bacterial sequences are those corresponding to *E. coli* RbsA, *T. litoralis* MalK, *S. typhimurium* HisP and the open reading frames 0796 and 1267 of *M. jannaschii*. The alignment was compiled with the program AMPS [73] and displayed with the program ALSCRIPT [74]. His-Loop, Histidine-Loop; Gln-Loop, Glutamine-Loop. (B) Sequence variability is plotted as a function of the residue position in the alignment. Minima in the peak indicate conserved areas. The five motifs indicated in the alignment correspond to the minima at positions 60, 120, 180, 210 and 240. ←

The perpendicular Arm-II contains the α-helical subdomain within which is situated the Signature Motif. The hinge region between the two arms contains both the His-Loop and the Gln-Loop (Fig. 3A).

Pure HisP was crystallised in the presence of 10 mM ATP and bound triphosphate was identified in the electron density maps. The environment of the bound ATP molecule is illustrated in Fig. 3B. The side chain atoms of residues contributing to the interaction with the ATP molecule are shown. The backbone of the Walker-A sequence, which interacts extensively with the phosphate groups, has been omitted for clarity. The ATP molecule forms contacts with the Walker-A (K45, S46, T47) and Walker-B (D178, E179) motifs that are typical of those observed in other ATP-binding proteins. The conserved histidine residue of the His-Loop (H211) also makes a contact with the γ-phosphate of ATP through a bound water molecule, but the Signature Motif of the monomeric HisP makes no contact with nucleotide. In addition, there are contacts with the conserved Gln-Loop (Q100 in HisP) and with an aromatic residue (Y16 in HisP) which is also well conserved across the ABC transporter family (position 24 of the alignment in Fig. 2A). The plane of this aromatic ring residue is parallel with the adenine ring of the nucleotide molecule and contributes to ATP binding. However, there are no extensive interactions with one side of the ATP molecule as clearly shown in Fig. 3A, and compared to other ATPases (e.g. F1-ATPase [26], adenylate kinase [27]) the bound nucleotide is rather exposed.

The L-shaped two-arm structure of monomeric nucleotide-binding domains has since been reflected in several other elucidated NBD structures (Table 2). Among these are several DNA-interacting NBD-like proteins, some of which are discussed in more detail

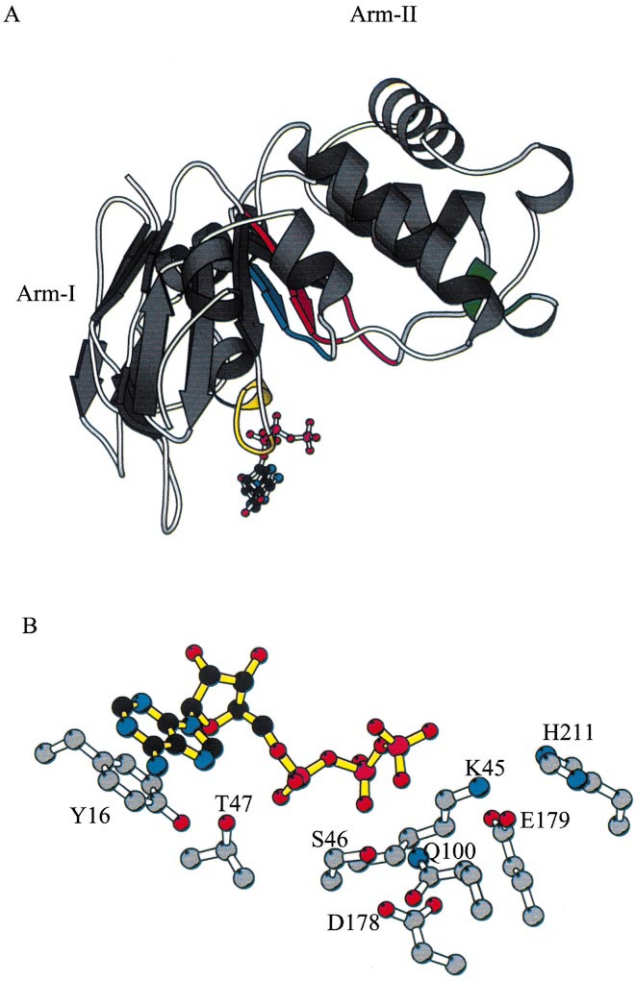

Fig. 3. (A) Structure of a monomeric nucleotide-binding domain from HisP. The two arms of the monomeric domain are indicated. α-Helices are shown as ribbons, while β-strands are displayed as arrows. Bound nucleotide (ATP) is displayed in ball-and-stick format. The conserved NBD motifs are shown in yellow (Walker-A), magenta (Gln-Loop), green (Signature Motif), red (Walker-B), and blue (His Loop). Coordinates obtained from 1BOU dataset at the Protein Data Bank [75]. (B) ATP-binding pocket of HisP. ATP and the side chains of residues forming interactions with the nucleotide are displayed in ball-and-stick format. Amino acid positions within the HisP sequence are indicated. For clarity the backbone atoms of the Walker-A motif are not displayed, although they interact with the α- and β-phosphate groups. This, and other molecular structure figures are displayed with the program Molscript [76]. Carbon atoms are displayed in grey (darker grey for ATP), oxygen atoms are in red, nitrogen in blue and phosphorus in pink.

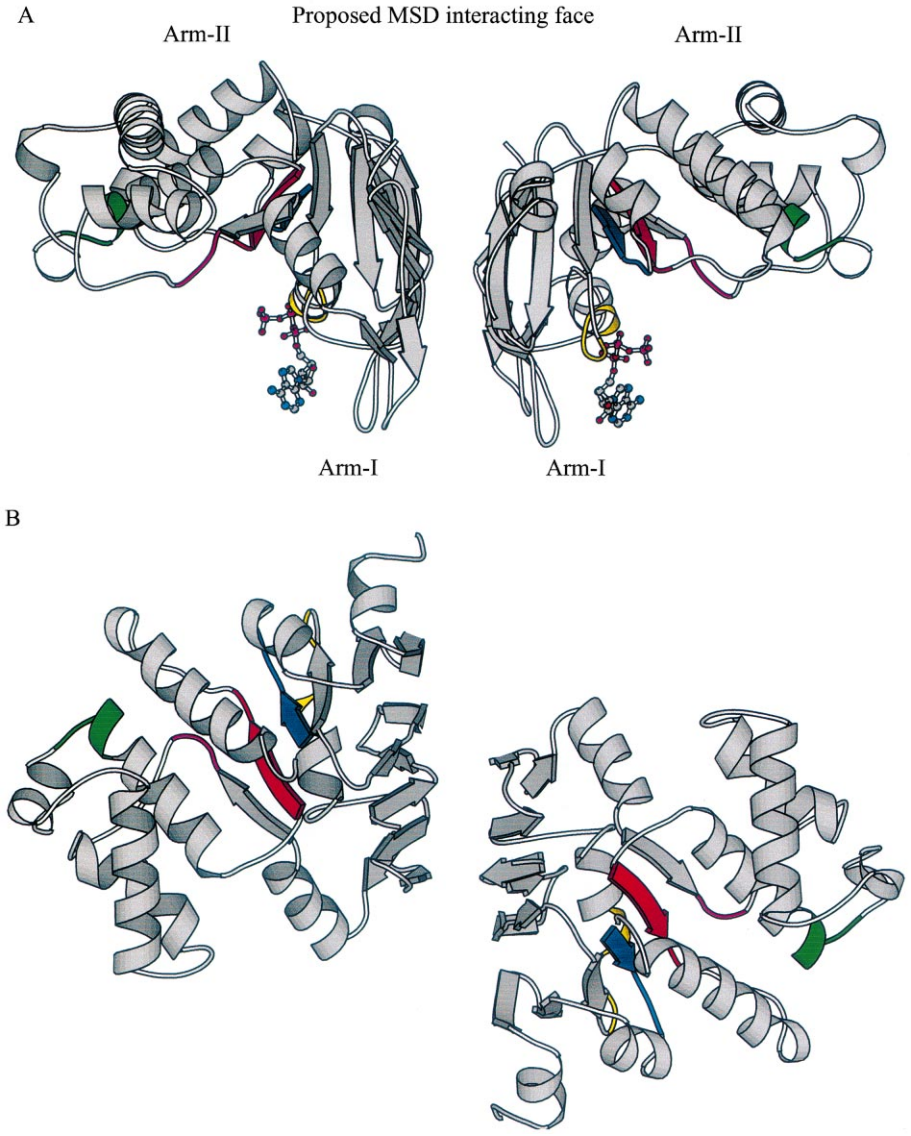

Fig. 4. Dimerisation of HisP. The crystallographic dimer of HisP [22] is displayed from two perpendicular orientations. The two arms of the molecule are indicated in A, in which the membrane-spanning domains are proposed to interact with Arm-II. B shows a view looking down on the two Arm-II lobes, showing the staggering of the β-sheet interface. Bound nucleotide and the conserved NBD sequence motifs are as in Fig. 3A.

below. Although MutS is mentioned in Table 2, and there are structural similarities with the NBD of HisP [28–30], the sequence homology between MutS and ABC domains is considerably harder to identify. It contains Walker-A and -B motifs, although the A motif is not the classical GxxGxGKS(S/T) as seen in Fig. 2A. Furthermore, the Signature Motif (LSGGQ) is not present within MutS sequences. These dissimilarities indicate that the ATPase domains of MutS are more distant relatives of ABC transporter NBDs and hence will not be discussed further in this review.

The structural changes involved in ATP binding and hydrolysis within a single NBD have been investigated crystallographically in studies of two *Methanococcus* NBDs, namely MJ0796 and MJ1267 [25,31], which provide a detailed description of subdomain movements and the reader is referred to discussions within these two extensive papers. However, as with all multidomain membrane proteins the over-

Table 2
Published structures of NBDs

NBD	Organism	Function	Resolution (Å)	Ref.
RbsA	*E. coli*	ribose uptake	2.5	[23]
HisP	*S. typhimurium*	histidine uptake	1.5	[22]
MalK	*T. litoralis*	maltose uptake	1.9	[21]
MJ0796	*Methanococcus jannaschii*	unknown	2.7	[31]
MJ1267	*M. jannaschii*	amino acid transport	1.6	[25]
Rad50	*P. furiosus*	double-strand repair of DNA	2.5	[32]
SMC	*T. maritima*	double-strand repair of DNA	3.1	[42]
MutS	*E. coli, Thermus aquaticus*	DNA mismatch repair	2.2	[28,29]

riding interest is the interaction between domains. In particular, as stated previously, the association of the NBDs is central to the catalytic cycle model of ABC transporters [15]. In this respect, the structures of HisP, MalK and Rad50 have caused considerable debate within the ABC transporter research community since they present dissimilar descriptions of the NBD:NBD interface [21,22,32]. This review will analyse the three 'dimer models' that have been presented and discuss ongoing efforts to resolve the confusion resulting from their diverse implications.

3. Alternative dimer interfaces of nucleotide-binding domains suggested by structural studies

3.1. HisP has a back-to-back structure

The crystallographic unit of HisP contains a dimer of two HisP monomers associated as shown in Fig. 4 [22]. The dimer has dimensions of width 90 Å × height 40 Å × thickness 60 Å. The dimer interface is comprised of residues contributed by three exposed β-strands of Arm-I, such that the two L-shape domains are in effect 'back-to-back' as displayed schematically in Fig. 7A. Among the buried residues are two aspartic acids which might not be an energetically favourable arrangement as there are no compensating charges at the interface. The common top surface in Fig. 4A, formed by the Arm-II structures, is proposed to interact with the MSDs of histidine permease transporter (HisQM). Within this dimer the two ATP molecules, which remain exposed, are separated by a distance of approx. 40 Å, while the two Signature Motifs are separated by a distance of approx. 80 Å (Table 3). Clearly, no direct interaction of the Signature Motifs with nucleotide can be hypothesised from this structure unless the loop has considerable flexibility (the distance is over 20 Å). Indeed the proposed function of the motif from these data is that it is required for the structural integrity of the NBD [22]. The His-Loops and Gln-Loops are also separated by greater than 50 Å, ruling out interactions between them. However, it is of interest that, within the crystal, a symmetry-related HisP molecule makes interactions with the bound ATP. Two positively charged residues just N-terminal to the Signature Motif of this symmetry-related HisP make contacts with the γ-phosphate. The significance of this interaction is unclear and it may merely be an effect of crystal packing.

3.2. MalK has an interlocking association

The structure of the MalK dimer from *Thermococcus litoralis* at 1.9 Å resolution [21] is shown in Fig. 5. In addition to the NBD, this protein contains an additional 140 amino acid regulatory domain that forms a barrel-shaped domain. If this domain is removed from the calculation, the dimer is approx. 50 Å in all dimensions, making it a more compact structure than the HisP dimer. The interface between the two domains contains a significant number of polar and aromatic residues, although direct interdomain contacts are absent. The interlocking domains of the two NBDs in the centre of Fig. 5A are not immediately identifiable and a more schematic representation is provided in Fig. 7B. Unlike HisP and Rad50 (see below) in which the two NBDs are perfectly symmetric (i.e. are related by 180°), in MalK the NBDs adopt a slightly imperfect symmetry. One suggestion that is consistent with this is that it re-

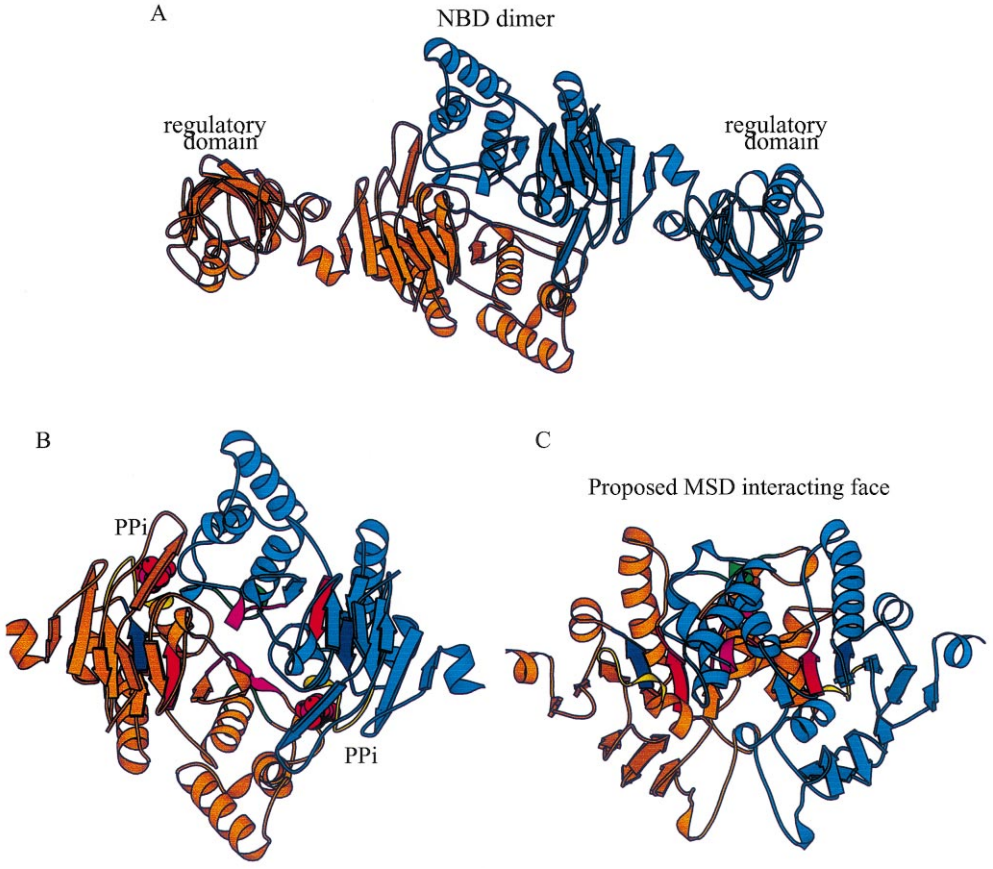

Fig. 5. The structure of MalK. The crystallographic dimer of MalK (PDB file 1G29) is displayed in ribbon format in A with the two additional regulatory domains at the extremity of the dimer. The regulatory domains are removed in B which views the ATPase dimer from the side proposed to interact with the membrane-spanning MalF and MalG subunits. The conserved sequence motifs indicated in earlier figures are coloured as before. The two bound pyrophosphate molecules are indicated in space-filling representation. A perpendicular view is presented in C. The top face of the dimer is proposed as the MalFG interacting face.

Table 3
Correlation of eukaryotic ABC transporter cross-linking data with prokaryotic ATPase structural studies

	Walker-A cross-linked residues[a]			β-Phosphate[c]	Lys:β-phosphate[d]	Sig:Sig[e]
	56–56[b]	52–56[b]	64–56[b]			
Rad50	33.4	30.2	39.2	26.9	24.4	24.9
MalK	40.1	41.8	30.0	31.6	33.5	16.4
HisP	43.0	46.6	33.1	48.4	48.7	82.0
ArsA	12.0	14.2	26.0	18.1	17.3	n/a

All distances are in Angstrom units.

[a]Residues that have been the subject of cross-linking analysis. For more details see Section 4.

[b]Distances between the Cα atoms of equivalent residues (numbers refer to the alignment in Fig. 2A). Thus, for example, 52–56 denotes that a cross-link has been observed in P-glycoprotein between residue 52 of NBD1 and residue 56 of NBD2. In the case of P-glycoprotein this equates to residues G427C cross-linked to residue C1074. The equivalent residues in Rad50 are 30.2 Å apart.

[c]Distance between the β-phosphate groups of ADP or ATP. For MalK the distance is the mean distance between the phosphate groups of pyrophosphate.

[d]Distance between the Walker-A lysine side chain amino group and the β-phosphate of nucleotide bound at the other NBD. The value given is an average of the two distances.

[e]Distance between the Ser-OH groups of the two signature motifs.

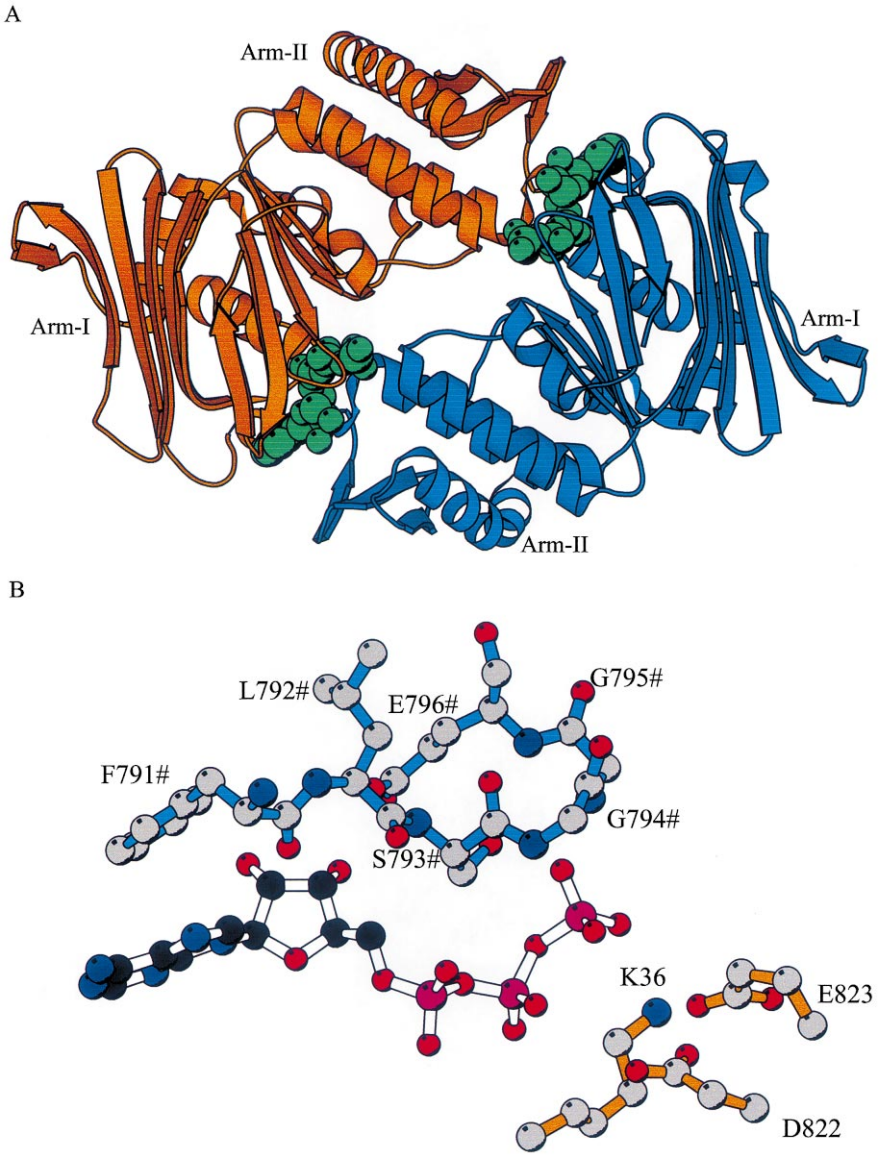

Fig. 6. Structure of a DNA repair ABC transporter-like domain, Rad50. (A) The dimeric structure of Rad50 is displayed in ribbon format. The two arms of the monomers are indicated. The two monomers are coloured in orange and blue. Two ATP molecules are sandwiched at the dimer interface and are coloured green and rendered in a space-filling style. PDB coordinate set 1F2U. (B) ATP bound at the Rad50 dimer interface is coordinated by residues from both monomers. ATP and protein atoms are displayed in ball-and-stick format. Side chains from the Walker-A and Walker-B motifs of one monomer are displayed with orange bonds, while those corresponding to the Signature Motif of the other monomer are displayed with blue bonds and denoted with a hash (#) symbol.

flects alternative conformations of the two NBDs which may be relevant in the transport cycle model of ABC transporters [15]. Although crystallised in the presence of ADP, no nucleotide could be unequivocally identified in the structure of MalK. Instead, pyrophosphate could be assigned to electron density close to the P-loop in positions equivalent those occupied by the α- and β-phosphate groups of ATP bound in HisP. The absence of an adenosine moiety, presumably due to disorder within the crystal, suggests that the MalK structure published may not correspond to the nucleotide-bound conformation [21].

Within the MalK structure the two Walker-A motifs are again approx. 40 Å from each other (Table 3). The absence of visibly bound nucleotide pre-

empts any measurements of inter-nucleotide distances. However, the two Signature Motifs are considerably closer across the interface separated by 18 Å, while the Gln-Loops approach as close as 4 Å consistent with a direct role in inter-domain communication for these two sequence motifs. Fig. 5C presents a view of the MalK dimer in which the MSDs (MalF and MalG) are proposed to interact with the top surface. It should be noted that the Signature Motif is present on this surface, thereby allowing conformational changes in this region to be conveyed to both the neighbouring NBD and also to the MSDs.

3.3. Rad50 forms an interlocking L-shape dimer

Rad50 (and indeed SMC – structural maintenance of chromosomes) are of considerable interest and have caused controversy as to whether they are a possible paradigm for ABC transporter NBDs. Both are approx. 1000 amino acid proteins whose N-terminal 150 amino acids contain a Walker-A motif and whose C-terminal 150 amino acids contain Walker-B, Signature and His-Loop motifs, thus identifying them as members of the ABC family, despite the lack of any MSDs. Sequence identity between full length Rad50 and SMC proteins is approx. 20%, although in the NBD-like region the identity is considerably greater. The crystal structure of Rad50 was obtained by co-expressing these N- and C-terminal 'NBD-like' sequences, while that of SMC was obtained by expressing the N- and C-terminal regions with a 14 amino acid linker region. In both cases the two half-domains formed the familiar NBD-type L-shaped domain. In addition, two molecules of the Rad50 NBD were found associated in a complex different to that seen for HisP and MalK [32].

The structure of the Rad50 NBD dimer from *Pyrococcus furiosus* is displayed in Fig. 6 [32]. The two L-shaped domains are clearly in an interlocking arrangement as shown schematically in Fig. 7C, which produces a dimer of dimensions of 60 Å×45 Å×90 Å. The effect of this interlocking is that two ATP (or indeed AMP-PNP as crystals were obtained with either nucleotide present) molecules are sandwiched between the two monomers and that bound nucleotide interacts not only with the classical Walker-A and -B motifs of one NBD, but also with the Signature Motif

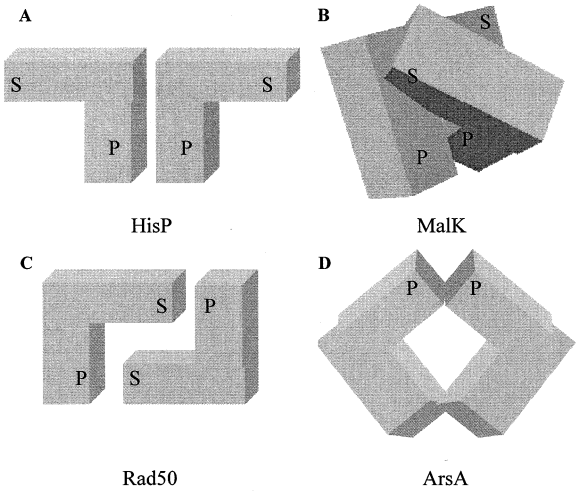

Fig. 7. Schematic representations of the NBD dimers. (A) HisP; (B) MalK; (C) Rad50; (D) ArsA. In each case the L-shapes represent the NBD, while 'S' and 'P' refer to the Signature Motif and the phosphate-binding loop (Walker-A) respectively. In the case of ArsA there is no Signature Motif.

of the 'opposite' NBD. This has the effect of supplying interactions with both sides of the ATP molecule, rather than only one side as seen in the monomeric NBD structures described above. This enclosure of nucleotide is presented in more detail in Fig. 6B in which the Walker-A lysine and Walker-B Asp/Glu pair are closely interacting with the β- and γ-phosphate of ATP, while the Signature Motif of the other monomer in the structure provides further interactions with the adenine ring as well as with the ribose and triphosphate moieties. It is worth noting that this orientation of NBDs is very similar to that predicted by Jones and George in a recent manuscript [33], although at an atomic level the exact details of their hypothesis are not borne out by the Rad50 structure. This close apposition of Signature Motifs with the ATP-binding pocket of the opposite NBD suggests a key role in inter-domain communication.

The three alternative dimer structures are illustrated for schematic purposes in Fig. 7A–C and pose the question: which of the dimer interfaces presents the likely mode of association between NBDs in an intact ABC transporter? The ensuing two sections will address this question from two viewpoints: (i) what *biochemical* evidence in prokaryotes supports particular dimer associations? (ii) what evidence in eukaryotic systems is there to support a particular structural model?

4. Association of nucleotide-binding domains in bacterial ABC proteins

4.1. Biochemical data pertaining to HisP

The main body of biochemical data pertinent to the structure of HisP concerns mutations within the protein which result in an alteration of the communication between HisP and other domains of the intact transporter. Thus, interactions between HisP and HisQM (the two MSDs) are disrupted, leading to ATPase activity in the absence of histidine [34]. Several of these 'uncoupling' mutations have been demonstrated to effect the interaction of HisP with the membrane-spanning protein HisQ as judged by co-purification and urea extractability experiments [35]. In co-purification experiments, cell membranes containing $HisQMP_2$ complexes were applied to metal affinity chromatography resin. In wild type complexes, in which the HisP protein had been engineered to contain a polyhistidine tail and thus bind to the resin, HisQ (and presumably HisM) remained non-covalently attached to HisP enabling it to be co-purified with the NBD. However, in $HisQMP_2$ complexes containing mutations within HisP that promote 'uncoupling', HisQ no longer co-eluted with HisP. In addition, urea extraction experiments demonstrated that it is far harder to remove wild type HisP from membranes containing $HisQMP_2$ complexes compared to membranes in which complexes contained HisP with 'uncoupling' mutations [35]. Both these approaches argue in favour of a reduced interaction between HisP and HisQ induced by these mutations. The 'uncoupling' residues all map to the exposed surface of Arm-II (Figs. 3A and 4A) and are consistent with this face interacting with HisQ (and presumably the other MSD, HisM). When mapped onto the MalK structure, two of these residues still lie on the proposed membrane-interacting face and are thus consistent with either the HisP or MalK model. Data supporting the accessibility of HisP from the periplasmic side of the membrane have been presented [36], and the proposed residue involved is on the upper surface of Arm-II [22]. This would again suggest that this upper surface is in contact with the MSDs. However, experiments on human P-glycoprotein have shown that the NBDs are not accessible from the extracellular face of the membrane which would argue against this proposal [37]. Further data proposing that the single tryptophan of HisP interacts with the membrane-spanning domains are not supported by the crystal structure of HisP since this residue is not exposed to the proposed membrane-interacting surface of the HisP dimer. Thus, while biochemical data pertinent to the structure of HisP suggest that the dimer model proposed [22] is a candidate for NBD:NBD interactions in ABC transporters, other structural models can also satisfy much of these data.

4.2. Biochemical data pertaining to MalK

In the MalK case there are considerable data regarding the association of subunits for the *E. coli* maltose transporter [38–40]. Most pertinently, cross-linking studies of residues in MalK have shown that A85 of *E. coli* MalK can be cross-linked to the equivalent residue in the adjacent MalK subunit when mutated to cysteine [39]. This residue (which is just C-terminal to the Gln Loop) maps onto the upper surface of the *T. litoralis* MalK dimer (Fig. 5C). The distance between the two equivalent residues (A91) is 17 Å which might suggest that the structure published is at odds with the cross-linking studies. However, the cross-linking was dependent on the nucleotide state of MalK (i.e. whether nucleotide was bound) and changes in the orientation of the two monomers upon nucleotide binding may allow a closer approach of these two residues. This cross-linking is consistent with the Rad50 dimer model as well, in which the equivalent residues (I143) are separated by 18 Å. In contrast, another residue which has been shown to induce dimerisation of MalK when mutated to cysteine [39], namely K106, is over 60 Å apart from the same residue in the opposite subunit in the *T. litoralis* MalK dimer. However, this residue is situated on the extreme edge of the MalK domain and the cross-linking data reported do not rule out *inter*molecular cross-linking. That is, when mutated to cysteine, K106 may form a disulphide bond with the equivalent residue of an adjacent MalFGK2 transport complex.

Cross-linking studies on MalK also impart information on the domain interface between the MSDs and the NBDs. In MalK the MSDs are encoded as two homologous polypeptides, namely MalF and

MalG. The cytoplasmic loops connecting putative transmembrane α-helices 4 and 5 of MalF and MalG contain a recently identified sequence motif [40], named the 'EAA' motif after the three amino acids which are well conserved across bacterial import ABC transporters. Genetic studies had demonstrated that non-functional $MalFGK_2$ transporters containing mutations within this motif could be rescued by suppressor mutations in the ABC-specific α-helical subdomain (Arm-II). While suggesting that there is an interaction between the EAA motif and this subdomain [40] these data cannot distinguish between a *direct* and an *indirect* (i.e. allosteric) interaction. However, when residues within the EAA motif were mutated to cysteine a direct interaction (i.e. formation of a disulphide bond) could be detected with cysteine residues introduced into the upper surface of the MalK dimer [39] (Fig. 5C). Therefore, these data suggest a direct contact between the MSDs and the upper surface of Arm-II (pictured in Fig. 3A). The data are consistent with the HisP and MalK dimer models, but *not* with the Rad50 structure in which the equivalent residues are not on the same face of the dimer.

Thus, the majority of published biochemical data on the maltose transporter support the published dimer structure [21] as being a very plausible model for the NBD:NBD interaction present in assembled ABC transporters.

4.3. Biochemical data pertaining to Rad50

In the case of Rad50 it was demonstrated in vitro that ATP was required for protein dimerisation consistent with the structural data locating ATP at the dimer interface. This is a significant point because it has been established for several ABC transporters that there is functional communication between the two NBDs [15–18,41]. Additional mutagenesis evidence suggests that this dimer represents a true physiological association state since mutation of the serine of the Signature Motif to arginine prevented ATP-dependent dimerisation [32]. This is consistent with the suggestion that mutation of a neutral residue to a positively charged one is sufficient to disrupt the protein:protein interaction. However, other lines of evidence might argue against the interlocking-L motif. The Rad50 dimer organisation was not observed in another DNA-interacting bacterial protein, namely SMC from *Thermotoga maritima*, which is involved in chromosomal segregation [42]. Despite their different functions, sequence analysis identifies Rad50 and SMC as members of the same protein family [43]. Members of this family are responsible for chromatid separation, chromosome condensation and double-strand break repair [43]. Unlike Rad50, the ABC domain of SMC remained monomeric in solution in the presence of ATP. Furthermore, SMC crystallised as a hexamer in the unit cell, regardless of the presence of ATP in the crystallisation conditions. The unusual oligomerisation of SMC, categorised by six NBD-like domains arranged head-to-tail, is rather difficult to rationalise with the Rad50 structure. It may be related to the high salt concentration (200 mM) required to maintain SMC in solution, which may cause altered protein:-protein and protein:ATP contacts. Additionally, within my laboratory we have also failed to demonstrate ATP-dependent dimerisation of human P-glycoprotein NBDs employing gel filtration chromatography (I.D.K., manuscript in preparation), while similar conclusions have been reached for the NBD of the haemolysin transporter (I.B. Holland, personal communication). This slightly confusing array of data on Rad50 indicates that the published structure may be the functionally relevant dimer in terms of double-strand break repair, it may not represent the physiological NBD:NBD dimer of intact ABC transporter complexes.

5. NBD interface probed in eukaryotic ABC transporters

Biochemical data on bacterial NBDs are unable to unambiguously determine which of the three proposed dimer organisations is most likely. The debate surrounding these structures has prompted investigations with full length eukaryotic ABC transporters in an attempt to shed light on the domain arrangement of the NBDs. Recent spectroscopic data on P-glycoprotein (P-gp) were obtained by Sharom and colleagues [44] by employing an elegant approach to label one NBD with the fluorescent sulphydryl reagent 2-(4′-maleimidylanilino)naphthalene-6-sulphonic acid (MIANS), and the other NBD with an-

other fluorescent sulphydryl chemical 7-chloro-4-nitrobenzo-2-oxa-1,3-diazole (abbreviated to NBD-Chloride). As the authors acknowledge [44], there are difficulties in interpreting these data since the detergent used in P-gp purification (3-[(3-cholamidopropyl)dimethylammonio]-1-propanesulphonate, CHAPS) and the Tris-based buffer both interact with and affect the fluorescent properties of NBD-Chloride. However, careful correction of fluorescence resonance energy transfer (FRET) measurements on the double-labelled protein either in membranes or solubilised in the detergent CHAPS indicated that the two fluorescent moieties were between 16 and 22 Å apart. Consideration of the size and flexibility of the two fluorophores allowed the authors to predict a distance between the two Walker-A cysteine residues of P-glycoprotein of 30–38 Å. Although these data might at first appear to support a Rad50-like association (in which the distance between the equivalent residues is 33 Å), it is consistent with the MalK orientation as well (in which the distance is 40 Å). The data appear to be inconsistent with the structure of HisP (even though the equivalent residues are only slightly over 40 Å apart) since the two fluorophores could not be 16–22 Å apart without colliding with the dimer interface.

Recently, two studies have provided insights into the association state of the NBDs of P-glycoprotein [45,46]. Both groups employed similar procedures to investigate potential cross-linking between cysteine residues in the opposite halves of P-gp. Human P-gp contains seven cysteine residues (which can be mutated to alanine or serine with only subtle pharmacological consequences [47,48]), two of which are located in the Walker-A motifs of the NBDs (Fig. 2A). The sequences around these two cysteines are GNSGCGKST and GSSGCGKST, with the two cysteines at positions C431 and C1074. Urbatsch et al. [46] demonstrated that these two cysteines form an *intramolecular* disulphide bridge in the presence of the oxidising agent copper phenanthroline, which was inhibited by preincubation with the sulphydryl reagent *N*-ethylmaleimide and completely reversed by incubation with the reducing agent dithiothreitol (DTT) [46]. Since the distance between a pair of cysteine residues involved in a disulphide bridge is 6–8 Å, the conclusion from this work is that the two NBDs face each other with the Walker-A motifs in close proximity. This would be reminiscent of the arrangement of domains in another transport ATPase ArsA (discussed below), rather than any of the NBD:NBD dimer models discussed. However, Loo and Clarke obtained a different result [45]. They employed a slightly different approach, although copper phenanthroline oxidation and analysis of mobility shifts by SDS–PAGE were employed to detect cross-linking. They made consecutive mutations to cysteine from residues 425–439 in NBD1 and attempted to cross-link them to C1074 in Walker-A of NBD2 (in an otherwise cysteine free P-gp). The only two double cysteine mutants that could be cross-linked were G427C with C1074 and L439C with C1074, although the equivalent mutations in the second NBD (i.e. G1070C and L1082C) failed to cross-link to C431. Oddly, C431 and C1074 did not form a disulphide bridge [45] as the work of Urbatsch and colleagues suggests [46]. The reasons for the discrepancies between the two sets of data are rather difficult to explain. Both groups employed similar oxidation protocols, although Loo and Clarke performed their screen on membranes from transiently transfected cells whereas Urbatsch et al. investigated protein purified from overexpressing yeast cultures. Whether these different environments could explain the disparity is unclear. With which structural models are the results consistent? To answer this question it is necessary to note that studies combining copper phenanthroline oxidation and bifunctional chemical cross-linkers indicate that the former reagent can cross-link cysteine residues as far apart as 17 Å [49,50]. Calculations of the distances between the side chains of the equivalent residues to those cross-linked in these studies are presented in Table 3. The distances involved are all over 25 Å which suggests that either the oxidation procedure forces conformational changes which enable cross-linking or that a different mode of NBD association may be required to explain the data. Furthermore, it is worth remembering that the fact that two cysteine residues can be cross-linked is a function not just of their separation, but also of their orientation, conformational freedom and reactivity [51]. In this respect the work of Urbatsch supports a degree of conformational flexibility since the C431 and C1074 single cysteine mutants were capable of forming *intermolecular* disulphide bonds. That is, one P-gp

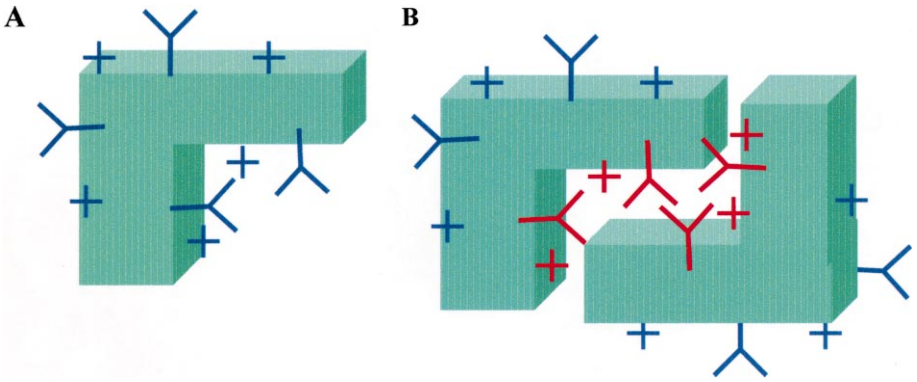

Fig. 8. Schematic representation of criteria employed to distinguish probable protein:protein interactions from crystallisation induced artefacts. (A) A single NBD is shown as an L-shape. Amino acids which are conserved across the ABC family are displayed as schematic 'Y' shapes, whereas variable amino acids are displayed as '+' symbols. Blue indicates amino acids that are solvent accessible. (B) The Rad50 dimer model is used for illustrative purposes. At the dimer interface some residues are no longer solvent accessible (coloured red). Many other residues show no change in accessibility (blue). The method presented in the text aims to determine if the conserved residues ('Y') are more frequently found at this dimer interface than non-conserved residues '+'.

molecule could be cross-linked to an adjacent P-gp molecule. Such an interaction might not be expected if the Walker-A motif cysteine residues were buried at the NBD dimer interface as the cross-linking data suggest [46].

One possibility raised by the structural studies is that some of the dimer models proposed are the result of crystallisation artefacts, i.e. that the association observed is due to intermolecular forces present during crystal formation. The question of identifying 'true' protein:protein interfaces from structure data is one which many structural biochemistry groups are devoting attention to [52,53]. I have recently applied a method presented by Elcock and MacCammon [52] to the dimeric structures of NBD proteins in an attempt to determine whether theoretical considerations can impact on our understanding of NBD:NBD associations. The reader is referred to the original source for a complete description of the method [52]. The premise of the approach is that two main criteria can be applied in determining a 'true' protein:protein contact from a crystallisation induced artefact. Firstly, the solvent accessible surface area (SASA) buried at the interface should exceed approx. 850 Å [53]. Secondly, residues at the interface should be more conserved within a protein family than those that are non-interfacial. A schematic illustrating this is presented in Fig. 8. The results of this analysis are presented in Table 4. For each protein four figures are given: (i) the SASA buried at the dimer interface, (ii) the mean sequence entropy of residues at the interface (sequence entropy being a measure of the degree of conservation of a residue, weighted for each residue's contribution to the SASA [52]), (iii) the mean sequence entropy of residues not at the interface, and (iv) the ratio of these values (i.e. (ii)/(iii), termed the 'entropy ratio'). As discussed in Elcock and MacCammon [52], the

Table 4
Characterisation of the NBD:NBD interfaces of published structures

NBD	Buried surface area[a]	⟨*S*⟩ interface[b]	⟨*S*⟩ non-interface	Entropy ratio[c]
MalK	approx. 3000	0.97	0.86	1.13
HisP	approx. 1000	1.22	0.57	2.13
Rad50	approx. 2500	0.61	1.10	0.56

[a]Surface area calculations (in Å^2) were performed using Xplor [72] with a probe radius of 1.6 Å.
[b]⟨*S*⟩, the sequence entropy, is calculated as described [52]. Interface residues were determined as those for which 50% of their accessible area was buried at the interface.
[c]The ratio of numbers in the previous two columns.

entropy ratio can be employed to discriminate between artefactual dimers and true protein:protein contacts with the following cutoffs:

entropy ratio < 0.9:	observed interface is a true protein:protein contact
$0.9 <$ entropy ratio < 1.1:	unambiguous assignment difficult
entropy ratio > 1.1:	observed interface is induced by crystallisation

According to these criteria only the Rad50 dimer represents a 'true' protein:protein interface, although the MalK interface would be classified as ambiguous. The HisP interface consists of residues no more conserved than non-interfacial residues and is considered by this analysis to be unlikely to represent a 'true' protein:protein dimer. In addition, the lower buried surface area makes this interface somewhat less plausible than those of Rad50 and MalK. The disadvantage with this analysis is that it is based upon the premise that interface residues are conserved because they are *structurally* important. If the interface also contains residues that are invariant because of *mechanistic* importance then the calculation may be biased towards such dimer interfaces. This criticism could easily be applied to the MalK and Rad50 structures since residues in the five conserved motifs (that are conserved for functional reasons) are interfacial. However, excluding residues within these motifs from the calculations returns an entropy ratio for Rad50 that is still indicative of a 'true' protein:protein interface. The MalK interface entropy ratio increases to 1.2, while that of HisP remains unchanged.

Current three-dimensional structural data on assembled ABC transporters are limited to electron microscopic studies of three eukaryotic proteins, namely P-gp [54], multidrug resistance associated protein (MRP) [55] and transporter associated with antigen presentation (TAP) (G. Verlade, R.C. Ford, personal communication). In all three cases the resolution of the data is at best 20–25 Å, which precludes any conclusive assignments of density as being NBDs. However, both Rad50 and MalK NBD dimers can be readily mapped onto the electron microscopic (EM) structure of TAP (G. Verlade, R.C. Ford, personal communication) whereas similar mapping for the HisP dimer results in a poorer fit.

6. Conclusions and perspectives

Perhaps a better understanding of the NBD:NBD dimer interface in ABC transporters will require higher resolution structural data either on an intact transporter or a fused two-NBD protein such as RbsA. Currently, resolution of this question may be closest at hand with continuing electron microscopic studies of P-glycoprotein, purified and reconstituted into lipid bilayers [56]. Ongoing three-dimensional reconstructions of this protein at between 10 and 15 Å resolution may well answer the question of domain:domain contacts [54]. Combinations of low resolution and high resolution data have previously been demonstrated to provide plausible models of membrane proteins. For example, the membrane-spanning pore formed by an oligomeric complex of *E. coli* haemolysin E has been observed by electron microscopy, but no high resolution structural data are available for this state. However, the monomeric toxin is soluble in aqueous solution and X-ray structural data have been obtained. Combining the two sets of data produces an atomic scale model for the associated toxin complex [57]. Thus, three-dimensional EM data on an entire ABC transporter (at 10–15 Å resolution) combined with X-ray structural data of NBDs (at atomic resolution) should enable such fitting procedures to determine both the NBD:NBD and NBD:MSD interfaces.

Thus far, this review has barely mentioned another membrane-spanning transport ATPase. The arsenic transporter, ArsAB [58], is comprised of two proteins; ArsB is a membrane-spanning domain, while ArsA is a cytoplasmic protein containing two ATPase domains with considerable homology to each other [59]. Although ArsAB shares some biochemical similarities with ABC transporters it is not a member of this superfamily, as ArsA does not possess the characteristic Signature Motif. However, recent high resolution structural data of the ArsA protein [60] may be informative to consider, since the ArsA ATPase 'dimer' is formed from a single polypeptide containing two homologous domains, rather than two separate proteins interacting as is the case for the dimer structures described earlier, and thus cannot be a crystallisation artefact. The two domains, pictured in Fig. 9, are arranged in a head-to-head, diamond-shaped orientation such that the Walker-A

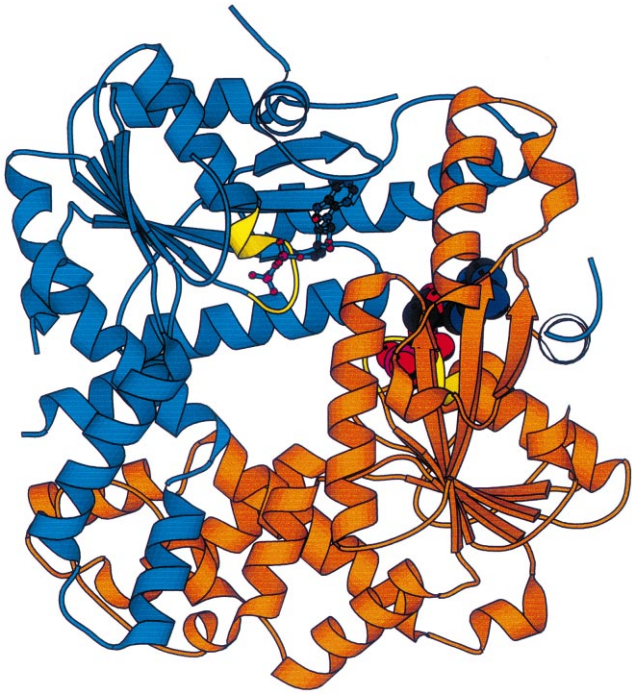

Fig. 9. Structure of a non-ABC transporter ATPase dimer. The crystal structure of ArsA (PDB coordinate set 1F48) is displayed in ribbon format, with the two homologous halves of the protein displayed in orange and blue. The Walker-A motifs are indicated in yellow. The two nucleotide molecules are shown in ball-and-stick or space-filling representation.

motifs of the two ATPase folds are in close apposition (Table 3). This orientation has been suggested to be a possible paradigm for ABC transporter NBD interactions and the close apposition of the two Walker-A sites is consistent with the P-gp cross-linking studies described above [45,46]. More recently, the same authors have obtained structural data for ArsA in a number of intermediate states in its catalytic cycle and have characterised the conformational changes that are apparent [61].

However, a further caveat is worth discussing. When considering the NBD:NBD interface an assumption is made that there is only one such interface in an intact transporter. There is at least one example where more than one NBD:NBD contact may be made in a functional protein, namely the sulphonylurea receptor (SUR) [62]. The latter is an octameric complex of four inwardly rectifying potassium channel (K_{IR}) subunits in association with four copies of an ABC transporter, namely SUR. The four K_{IR} subunits are presumed to form a tetrameric, potassium selective pore around a central axis as has been shown crystallographically for a bacterial potassium channel [63], while the four SUR subunits are proposed to form a larger ring around the exterior of the K_{IR} complex. Within this octameric assembly there will undoubtedly be interactions between NBDs within an SUR molecule (i.e. *intramolecular*) and contacts between NBDs in adjacent SUR molecules (i.e. *intermolecular*). It is conceivable that the intramolecular NBD:NBD interface may be substantially different in structure from the intermolecular NBD:NBD interface. In the context of multiple interactions of NBDs it is also worth noting that within the genome of *Drosophila melanogaster* [64] there is a gene (cg17338) whose sequence consists of four NBDs together with four blocks of predicted membrane-spanning α-helices. The topology of the protein predicted by the program MEMSAT [65] appears to be $(MSD\text{-}NBD\text{-}MSD\text{-}NBD)_2$ (Kerr, unpublished observations). Thus, in at least two cases there is likely to be more that one mode of association between NBDs. Therefore, it may be imprudent to believe that we are only searching for a unique NBD:NBD interface to enable us to understand their intercommunication. Indeed as work on ArsA and two methanotrophic bacterial NBDs demonstrates there are considerable conformational changes accompanying ATP binding, hydrolysis and phosphate release [25,31,61]. Whether these could be of sufficient magnitude to alter the NBD:NBD interface from one resembling MalK to one resembling Rad50 for example remains to be determined.

Finally, although future structural studies may identify the NBD:NBD interface in ABC transporters there will still be intense activity to determine exactly the nature of any dynamic interactions occurring at this interface to effect not only conformational changes in the adjacent NBD, but also how NBD:NBD communication is related to NBD:MSD communication. The recent example of the voltage-gated potassium channel is worth highlighting. The crystal structure of a bacterial potassium channel [63] has intensified research aimed at elucidating the conformational changes necessary to interconvert closed and open conformations [66]. A static picture of an entire ABC transporter may be the launch point for similar investigations into ABC transporter conformational change.

Acknowledgements

I would like to thank Richard Callaghan, Andrew Taylor, Janet Storm and Mark Gabriel for their helpful comments on draft versions of the manuscript, and also Peter Jones and Barry Holland for helpful discussions.

Note added in proof

The ABC transporter community has recently been excited by the publishing of the first 3D crystal structure of an ABC transporter [77]. MsbA, involved in lipid A membrane-insertion [78], is a half transporter, i.e. it is comprised of a single NBD and a single MSD and presumably functions as a homodimer. The structure of MsbA, determined to 4.5 Å, is a major breakthrough in the understanding of ABC transporters. It confirms the long-held hypothesis that the transmembrane domains are compromised of α-helices, and provides evidence for an additional α-helical domain linking the MSDs to the NBDs. These linker domains are presumably involved in the conformational coupling that accompanies allocrite binding and transport.

However, in terms of revealing the interaction between NDBs in an intact transporter, MsbA fails to provide the answer for two significant reasons. Firstly, the NDBs of MsbA are not completely resolved in the structure. In particular, although Arm-II appears in the electron density maps there is little data for Arm-I, with some 75 amino acids unresolved. Secondly, although the crystal structure of MsbA does indeed reveal a dimer, there are considerable grounds for believing that this may not represent the physiologically relevant dimeric state, as discussed in an overview of the structure [79]. This short addendum does not allow for a detailed discussion of the matter and the reader is referred to the original manuscripts [77,79].

In conclusion, although the MsbA structure [77] significantly enhances our understanding of ABC transporters, it leaves a number of questions unanswered, including those regarding NBD:NBD association and communication. There seems little doubt that MsbA will serve as a catalyst for renewed investigations to address these questions, and probe new areas of research opened up by this impressive advance.

References

[1] C.F. Higgins, Annu. Rev. Cell Biol. 8 (1992) 67–113.
[2] Biochim. Biophys. Acta 1461 (1999) part 2.
[3] Microbiol. Rev. 152 (2001) parts 3–4.
[4] K.J. Linton, C.F. Higgins, Mol. Microbiol. 28 (1998) 5–13.
[5] Y. Quentin, G. Fichant, F. Denizot, J. Mol. Biol. 287 (1999) 467–484.
[6] B.E. Bauer, H. Wolfger, K. Kuchler, Biochim. Biophys. Acta 1461 (1999) 217–236.
[7] R. Sanchez-Fernandez, T.G. Emyr Davies, J.O.D. Coleman, P.A. Rea, J. Biol. Chem. 276 (2001) 30231–30244.
[8] M. Dean, A. Rzhetsky, R. Allikmets, Genome Res. 11 (2001) 1156–1166.
[9] P.M. Jones, A.M. George, J. Membr. Biol. 166 (1998) 133–147.
[10] I.B. Holland, M.A. Blight, J. Mol. Biol. 293 (1999) 381–399.
[11] C. Martin, G. Berridge, C.F. Higgins, P. Mistry, P. Charlton, R. Callaghan, Mol. Pharmacol. 58 (2000) 624–632.
[12] J.C. Spurlino, G.-Y. Lu, F.A. Quiocho, J. Biol. Chem. 266 (1991) 5202–5219.
[13] C.E. Liu, P.Q. Liu, A. Wolf, E. Lin, G.F. Ames, J. Biol. Chem. 274 (1999) 739–747.
[14] J.R. Riordan, J.M. Rommens, B. Kerem, N. Alon, R. Rozmahel, Z. Grzelczak, J. Zielenski, S. Lok, N. Plavsic, J.L. Chou et al., Science 245 (1989) 1066–1073.
[15] A.E. Senior, M.K. al Shawi, I.L. Urbatsch, FEBS Lett. 377 (1995) 285–289.
[16] Y. Hou, L. Cui, J.R. Riordan, X. Chang, J. Biol. Chem. 275 (2000) 20280–20287.
[17] J.T. Karttunen, P.J. Lehner, S.S. Gupta, E.W. Hewitt, P. Cresswell, Proc. Natl. Acad. Sci. USA 98 (2001) 7431–7436.
[18] L. Aleksandrov, A. Mengos, X. Chang, A. Aleksandrov, J.R. Riordan, J. Biol. Chem. 276 (2001) 12918–12923.
[19] C.A. Hrycyna, M. Ramachandra, U.A. Germann, P.W. Cheng, I. Pastan, M.M. Gottesman, Biochemistry 38 (1999) 13887–13899.
[20] J.E. Walker, M. Saraste, M.J. Runswick, N.J. Gay, EMBO J. 1 (1982) 945–951.
[21] K. Diederichs, J. Diez, G. Greller, C. Muller, J. Breed, C. Schnell, C. Vonrhein, W. Boos, W. Welte, EMBO J. 19 (2000) 5951–5961.
[22] L.W. Hung, I.X. Wang, K. Nikaido, P.Q. Liu, G.F. Ames, S.H. Kim, Nature 396 (1998) 703–707.
[23] S. Armstrong, L. Tabernero, H. Zhang, M. Hermodsen, C. Stauffacher, Pediatr. Pulmonol. 17 (1998) 91–92.
[24] R.E. Kerppola, V.K. Shyamala, P. Klebba, G.F.-L. Ames, J. Biol. Chem. 266 (1991) 9857–9865.
[25] N. Karpowich, O. Martsinkevich, L. Millen, Y.R. Yuan, P.L. Dai, K. MacVey, P.J. Thomas, J.F. Hunt, Structure 9 (2001) 571–586.

[26] J.P. Abrahams, A.G. Leslie, R. Lutter, J.E. Walker, Nature 370 (1994) 621–628.
[27] C. Vonrhein, G.J. Schlauderer, G.E. Schulz, Structure 3 (1995) 483–490.
[28] M.H. Lamers, A. Perrakis, J.H. Enzlin, H.H.K. Winterwerp, N. de Wind, T.K. Sixma, Nature 407 (2000) 711–717.
[29] G. Oblomova, C. Ban, P. Hsieh, W. Yang, Nature 407 (2000) 703–710.
[30] T.K. Sixma, Curr. Opin. Struct. Biol. 11 (2001) 47–52.
[31] Y.R. Yuan, S. Blecker, O. Martsinkevich, L. Millen, P.J. Thomas, J.F. Hunt, J. Biol. Chem. 276 (2001) 32313–32321.
[32] K.P. Hopfner, A. Karcher, D.S. Shin, L. Craig, L.M. Arthur, J.P. Carney, J.A. Tainer, Cell 101 (2000) 789–800.
[33] P.M. Jones, A.M. George, FEMS Microbiol. Lett. 179 (1999) 187–202.
[34] V. Petronilli, G.F. Ames, J. Biol. Chem. 266 (1991) 16293–16296.
[35] P.Q. Liu, C.E. Liu, G.F. Ames, J. Biol. Chem. 274 (1999) 18310–18318.
[36] V. Baichwal, D. Liu, G.F.-L. Ames, Proc. Natl. Acad. Sci. USA 90 (1993) 620–624.
[37] E.J. Blott, C.F. Higgins, K.J. Linton, EMBO J. 18 (1999) 6800–6808.
[38] M. Ehrmann, R. Ehrle, E. Hofmann, W. Boos, A. Schlosser, Mol. Microbiol. 29 (1998) 685–694.
[39] S. Hunke, M. Mourez, M. Jehanno, E. Dassa, E. Schneider, J. Biol. Chem. 275 (2000) 15526–15534.
[40] M. Mourez, M. Hofnung, E. Dassa, EMBO J. 16 (1997) 3066–3077.
[41] C. Proff, R. Kolling, Mol. Gen. Genet. 264 (2001) 883–893.
[42] J. Lowe, S.C. Cordell, F. van den Ent, J. Mol. Biol. 306 (2001) 25–35.
[43] N. Cobbe, M.M. Heck, J. Struct. Biol. 129 (2000) 123–143.
[44] Q. Qu, F.J. Sharom, Biochemistry 40 (2001) 1413–1422.
[45] T.W. Loo, D.M. Clarke, J. Biol. Chem. 275 (2000) 19435–19438.
[46] I.L. Urbatsch, K. Gimi, S. Wilke-Mounts, N. Lerner-Marmarosh, M.E. Rousseau, P. Gros, A.E. Senior, J. Biol. Chem. 276 (2001) 26980–26987.
[47] T.W. Loo, D.M. Clarke, J. Biol. Chem. 270 (1995) 843–848.
[48] A.M. Taylor, J. Storm, K.J. Linton, M. Gabriel, E.J. Blott, C. Martin, C.F. Higgins, P. Mistry, P. Charlton, R. Callaghan, Br. J. Pharmacol. (2001) in press.
[49] M. Hashimoto, E. Majima, S. Goto, Y. Shinohara, H. Terada, Biochemistry 38 (1999) 1050–1056.
[50] E. Majima, K. Ikawa, M. Takeda, M. Hashimoto, Y. Shinohara, H. Terada, J. Biol. Chem. 270 (1995) 29548–29554.
[51] J. Sun, C.R. Kemp, H.R. Kaback, Biochemistry 37 (1998) 8020–8026.
[52] A.H. Elcock, J.A. McCammon, Proc. Natl. Acad. Sci. USA 98 (2001) 2990–2994.
[53] H. Ponstingl, K. Henrick, J.M. Thornton, Proteins 41 (2000) 47–57.
[54] M.F. Rosenberg, R. Callaghan, R.C. Ford, C.F. Higgins, J. Biol. Chem. 272 (1997) 10685–10694.
[55] M.F. Rosenberg, Q. Mao, A. Holzenburg, R.C. Ford, R.G. Deeley, S.P. Cole, J. Biol. Chem. 276 (2001) 16076–16082.
[56] R. Callaghan, G. Berridge, D.R. Ferry, C.F. Higgins, Biochim. Biophys. Acta 1328 (1997) 109–124.
[57] A.J. Wallace, T.J. Stillman, A. Atkins, S.J. Jamieson, P.A. Bullough, J. Green, P.J. Artymiuk, Cell 100 (2000) 265–276.
[58] A.R. Walmsley, T. Zhou, M.I. Borges Walmsley, B.P. Rosen, J. Biol. Chem. 274 (1999) 16153–16161.
[59] D. Gatti, B. Mitra, B.P. Rosen, J. Biol. Chem. 275 (2000) 34009–34012.
[60] T. Zhou, S. Radaev, B.P. Rosen, D.L. Gatti, EMBO J. 19 (2000) 4838–4845.
[61] T. Zhou, S. Radaev, B.P. Rosen, D.L. Gatti, J. Biol. Chem. 276 (2001) 30414–30422.
[62] J. Bryan, L. Aguilar-Bryan, Biochim. Biophys. Acta 1461 (1999) 285–303.
[63] D.A. Doyle, J.M. Cabral, R.A. Pfuetzner, A. Kuo, J.M. Gulbis, S.L. Cohen, B.T. Chait, R. MacKinnon, Science 280 (1998) 69–77.
[64] M.D. Adams, S.E. Celniker, R.A. Holt, C.A. Evans, J.D. Gocayne, P.G. Amanatides, S.E. Scherer, P.W. Li, R.A. Hoskins, R.F. Galle et al., Science 287 (2000) 2185–2195.
[65] D.T. Jones, W.R. Taylor, J.M. Thornton, FEBS Lett. 339 (1994) 269–275.
[66] M.S. Sansom, Curr. Biol. 10 (2000) R206–R209.
[67] S.V. Ambudkar, S. Dey, C.A. Hrycyna, M. Ramachandra, I. Pastan, M.M. Gottesman, Annu. Rev. Pharmacol. Toxicol. 39 (1999) 361–398.
[68] H.W. van Veen, R. Callaghan, L. Socenteantu, A. Sardini, W.N. Konings, C.F. Higgins, Nature 391 (1998) 291–295.
[69] I.B. Holland, B. Kenny, M. Blight, Biochimie 72 (1990) 131–141.
[70] H. Sun, R.S. Molday, J. Nathans, J. Biol. Chem. 274 (1999) 8269–8281.
[71] B. Lankat Buttgereit, R. Tampe, FEBS Lett. 464 (1999) 108–112.
[72] A.T. Brunger, X-PLOR Version 3.1. A system for X-ray crystallography and NMR, Yale University Press, New Haven, CT, 1992.
[73] G.J. Barton, Methods Mol. Biol. 25 (1994) 327–347.
[74] G.J. Barton, Protein Eng. 6 (1993) 37–40.
[75] F.C. Bernstein, T.F. Koetzle, G.J. Williams, E.E. Meyer Jr., M.D. Brice, J.R. Rodgers, O. Kennard, T. Shimanouchi, M. Tasumi, J. Mol. Biol. 112 (1977) 535–542.
[76] P.J. Kraulis, J. Appl. Crystallogr. 24 (1991) 946–950.
[77] G. Chang, C.B. Roth, Science 293 (2001) 1793–1800.
[78] Z. Zhou, K.A. White, C. Polissi, C. Georgopoulos, C.R. Raetz, J. Biol. Chem. 273 (1998) 12466–12475.
[79] C.F. Higgins, K.J. Linton, Science 293 (2001) 1782–1784.